PHYSICAL REVIEW B
CONDENSED MATTER

THIRD SERIES, VOLUME 31, NUMBER 9 1 MAY 1985

Melting-induced electron localization: ^{133}Cs NMR study of solid and liquid CsAu

R. Dupree and D. J. Kirby*
Department of Physics, University of Warwick, Coventry, Warwickshire CV47AL, England

W. W. Warren, Jr.
AT&T Bell Laboratories, Murray Hill, New Jersey 07974
(Received 27 December 1984)

We describe a ^{133}Cs NMR study of the ionic intermetallic semiconductor CsAu and the transition to its saltlike liquid state. Measurements of the resonance shift and nuclear relaxation rates extend from room temperature through the melting point to 650 and 700 °C, respectively. A strongly-temperature-dependent spin-lattice relaxation rate and accompanying shift in the solid are attributed to extrinsic, nondegenerate, delocalized electrons which are excited from a donor band about 0.25 eV below the conduction band. A sharp 25-fold increase in the relaxation rate at the melting point is not accompanied by a similar jump in the shift, showing that the conduction electrons become localized immediately upon passing to the liquid state.

I. INTRODUCTION

The unusual liquid-state properties of the intermetallic compound CsAu have drawn considerable attention to this material during the last ten years. Whereas liquid cesium and liquid gold each exhibit the properties of nearly-free-electron metals, their equiatomic solution closely resembles a molten salt such as CsCl. Hoshino *et al.*,[1,2] for example, observed dc conductivities around 3 Ω^{-1}cm^{-1}, a typical value for the conductivity of a molten salt, and subsequent electromigration experiments[3] confirmed that the conductivity mechanism is indeed ionic. Magnetic,[4] structural,[5] and thermodynamic data[6,7] also support the characterization of CsAu as a molten salt. Addition of sufficient amounts of excess Cs to CsAu eventually leads to a continuous metal-nonmetal transition similar to those occurring in liquid cesium-cesium halide solutions.[8]

Solid CsAu forms in the CsCl structure typical of ionic materials[9] and has an optical band gap of 2.6 eV at room temperature.[10] A number of recent band-structure calculations[11–13] agree that CsAu should be a semiconductor with a high degree of charge transfer from the cesium to the gold. In practice the solid compound is very difficult to obtain close to exact stoichiometry and Spicer *et al.*[10] and Wooten and Condas[14] were able to obtain only extrinsic *n*-type semiconducting material with a relatively large, weakly-temperature-dependent conductivity ($\sigma > 4\ \Omega^{-1}$ cm^{-1}. They ascribed this conductivity to donor states associated with excess cesium. Overhof *et al.*[12] suggested that the excess cesium forms a donor band overlapping the bottom of the conduction band. Tinelli and Holcomb[15] carried out an NMR and x-ray investigation at room temperature and they also interpreted their results in terms of doping by excess cesium. They concluded that their best sample contained 10^{15}–10^{16} excess cesium atoms per cm^3.

In a previous NMR investigation,[16] we approached the study of molten CsAu by way of the Cs-Au liquid-alloy system and the metal-nonmetal transition that occurs as the cesium concentration is varied. In the present study we focus on the temperature-dependent properties of nearly stoichiometric solid CsAu and on the changes associated with the loss of long-range order at the melting transition. We shall show that CsAu behaves as an extrinsic semiconductor up to the melting point but a significant change occurs on melting whereupon the electrons become much more strongly localized. To reach this conclusion we exploit the high sensitivity of NMR to the local static and dynamic magnetic (hyperfine) fields produced by the spins of localized and itinerant electrons. Our measurements include the ^{133}Cs resonance shift and nuclear relaxation rates, and they extend from room temperature through the melting point ($T_m = 590$ °C) to 700 °C.

The organization of this paper is as follows. We describe our measurement techniques and our methods of sample preparation and confinement in Sec. II. The experimental results for solid and liquid CsAu are presented in Sec. III and they are discussed in Sec. IV in terms of hyperfine interactions with nondegenerate conduction electrons. Finally we summarize briefly the main observations and conclusions of the work in Sec. V.

II. EXPERIMENTAL METHODS

These experiments were conducted in separate laboratories at the University of Warwick and AT&T Bell Laboratories. The sample preparation procedures and measurement techniques differed only in minor details and in the following discussion we do not distinguish between methods employed in the two locations.

We carried out these measurements with pulsed NMR techniques at various frequencies in the range 9—13 MHz using electromagnets and 25—40 MHz using a superconducting magnet. The ^{133}Cs resonant field at low frequencies was determined by sweeping the magnetic field through resonance while integrating the free induction decay with a boxcar integrator.[17] The ^{133}Cs shift was measured relative to an aqueous CsCl solution (corrected to infinite dilution[18]) mounted outside the furnace. In the superconducting magnet we employed the same principle by sweeping the frequency instead of the field. Alternatively in some cases, we measured the resonant frequency directly from the beats in an off-resonance free induction decay. Relaxation times were measured using a $\pi-\pi/2$ sequence for the spin-lattice relaxation time, T_1, a $\pi/2-\pi$ sequence for the transverse relaxation time, T_2, and a $\pi/2$ pulse for T_2^*, the free-induction-decay lifetime.

The extreme reactivity of cesium at the necessary high temperatures presented a severe problem for sample confinement. A number of different types of sample cell were tried and a relatively successful version is shown in Fig. 1.[19] A sapphire tube of ~1-mm wall thickness used to contain the sample was bonded to a niobium collar and sealed using a reusable molybdenum cone compression joint. The principal difficulty with this design was providing a sapphire-niobium bond that was both vacuum tight and resistant to attack by cesium vapor. For the cell shown in Fig. 1, the bond was made using alternating 0.025-mm foil strips of nickel and titanium in the atomic ratio 50:50 to achieve a total thickness of ~0.25 mm. This was force-fit under the niobium collar and heated in a vacuum of 10^{-6} Torr to a temperature of 1360 °C for 2 min. Good cells, when tested, gave a helium-gas leak rate at room temperature less than 10^{-10} Torr l/s. Lucalox and BeO gave similar results and were sometimes used in place of sapphire in the cell construction. For all cells the niobium/sapphire bond was attacked slowly by the cesium vapor leading eventually to leakage of cesium from the cell.

The samples were prepared in a helium dry box where they were filled with the required amounts of cesium and gold and, in most cases, sealed immediately. The accuracy of weighing and handling losses were such that the uncertainty in composition was 0.1% in the atomic fraction x (Cs_xAu_{1-x}) or 0.3% on the excess metal scale y [$Cs_y(CsAu)_{1-y}$]. Before it was sealed, one sample made from a nominal composition $Cs_{0.505}Au_{0.495}$ was reacted at 260 °C for 8 h, while pumping to remove the excess cesium. As noted by Tinelli and Holcomb[15] the nuclear-spin-lattice relaxation in solid CsAu is very sensitively increased by excess cesium and this was our most stoichiometric sample by this criterion.

Furnaces of standard design[19,20] provided temperatures

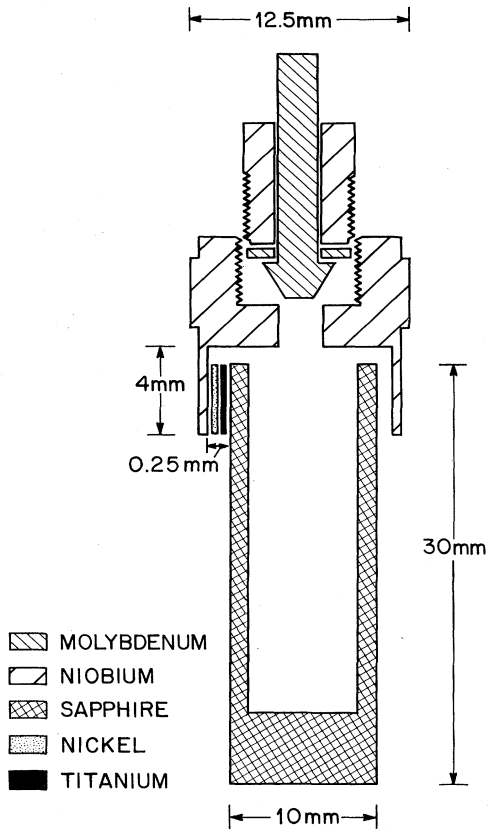

FIG. 1. Sample cell for CsAu NMR studies. The sapphire crucible is bonded to the niobium closure assembly with a nickel-titanium braze as discussed in text. Molybdenum cone compression seal closes the cell after filling with cesium and gold.

up to 700 °C with temperature gradients smaller than 5 °C over the 2-cm cell length. Because the sample cell assemblies contained niobium and molybdenum it was important to ensure that the furnace atmosphere was oxygen free. The furnaces were therefore enclosed in vacuum-tight containers which could be back-filled with argon gas to reduce the thermal time constant. The molybdenum NMR coil was mounted in high-temperature cement[21] and fitted closely around the sapphire cell. For the superconducting system, the sample cell could not be mounted perpendicular to the magnetic field so we used a saddle-shaped NMR coil.[22] The temperature was measured using a chromel-alumel thremocouple mounted 1—2 mm from the base of the sample cell. This thermocouple was also used to regulate the temperature of the sample. The uncertainty in sample temperature was less than 5 °C.

III. EXPERIMENTAL RESULTS

Figure 2 shows the relaxation rates T_1^{-1} and T_2^{-1} plotted against temperature for several samples all nominally $Cs_{0.50}Au_{0.50}$. In every case, the data in the solid were taken after heating the sample above the melting temperature to ensure homogeneity. Data taken during additional

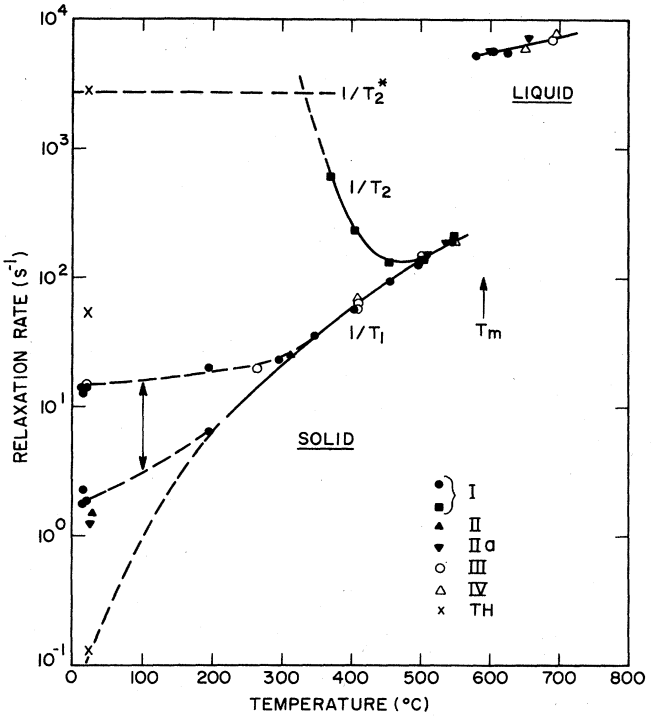

FIG. 2. Semilogarithmic plot of ^{133}Cs relaxation rates $1/T_1$ and $1/T_2$ versus temperature for solid and liquid CsAu. Samples I, II, and IIa (closed symbols) and samples III and IV (open symbols) were prepared and measured at AT&T Bell Laboratories and the University of Warwick, respectively. For sample I below 300 °C, both components of the relaxation are indicated. Room temperature $1/T_2^*$ and $1/T_1$ values denoted *TH* (x) are quoted from Ref. 15.

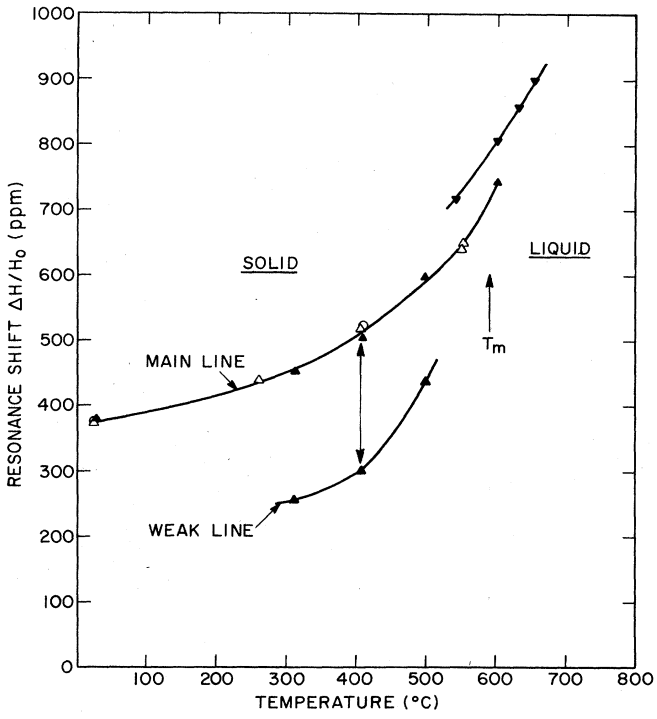

FIG. 3. ^{133}Cs resonance shifts $\Delta H/H_0$ versus temperature for solid and liquid CsAu. Sample designations are as in Fig. 2. Shift values for the weak second line of sample II are indicated by the lower curve.

thermal cycles were reproducible within the experimental uncertainty. For all samples T_1^{-1} increases strongly with temperature and undergoes a further large ($\sim$25 fold) increase on melting. Above about 300 °C, T_1^{-1} values for the various samples indicated in Fig. 2 agree within experimental error but below this temperature the results are sample dependent, presumably because of small departures from stoichiometry. Sample I prepared in the usual manner from stoichiometric proportions gave a double exponential for the magnetization recovery below about 220 °C and both the long and short relaxation rates are shown. Both components were reproducible upon separate heatings. Our "best" sample (sample II) was prepared, as indicated above, by pumping the excess cesium from a mixture initially slightly Cs rich. This sample exhibited only a single exponential relaxation component, the smallest shift in the liquid of any sample, and practically the longest room temperature relaxation rate. Also shown in Fig. 2 are data for the same sample after addition of 10 mg of gold (sample IIa), which should therefore be gold rich. It can be seen that there is relatively little difference between the longer relaxation rate for sample I and those for samples II and IIa at room temperature. Even these differences disappeared at higher temperatures in the solid. The room temperature relaxation rates of the two best samples of Tinelli and Holcomb are also shown in Fig. 2, and it can be seen that the rates for all our samples fall between theirs. However we should point out that we were unable to obtain homogeneous samples by solid state reaction at 300 °C, the method used by Tinelli and Holcomb.

The value of T_2^*, the free induction decay lifetime, is much shorter at room temperature than calculated from the second moment, indicating that at this temperature, the line is inhomogeneously broadened. Motional narrowing starts at about 300 °C and by about 450 °C, $T_2 = T_1$. At temperatures between the motional narrowing temperature and the melting point, the presence in most of our samples of a small amount of a second phase is revealed by a weak second line at a smaller shift than the main line. The relaxation rates for this weaker line were not measured.

The variation of the shift with temperature is shown in Fig. 3. At room temperature, the shift value 375±15 ppm, is comparable with those observed[23] for CsI, 274 ppm, and CsCl, 228 ppm. By 300 °C it has increased to 450 ppm and then rises more rapidly to reach 700 ppm just below the melting point. The shift continues to increase steadily up to the highest temperature measured but, in contrast to the relaxation, there is only a very small discontinuity on melting.

IV. DISCUSSION

A. Solid CsAu

The relaxation rates observed for CsAu, particularly at high temperatures, are much higher than those measured

for stoichiometric cesium halides. The ^{133}Cs $1/T_1$ value in solid CsI,[24] for instance, is about 0.1 s^{-1} near the melting point compared with 200 s^{-1} observed in CsAu. In fact the relaxation in CsAu at high temperatures is far too strong to be of either nuclear dipole-dipole or quadrupolar origin (^{133}Cs has a very small electric quadrupole moment) and must therefore arise from interaction between unpaired electron spins and the nuclear spins.

One possibility is that these unpaired electrons are present in the form of paramagnetic localized centers, such as neutral atoms or F centers. In such a case the dominant relaxation mechanism would be the dipolar coupling between the electron and nuclear spins.[25] For dilute (isolated) centers, this mechanism gives a relaxation rate,[26]

$$1/T_1 = 4\pi NbD \ , \tag{1}$$

where N is the number of localized paramagnetic centers per unit volume, D is the spin diffusion constant, and b is a length of the order of the lattice spacing. A shift is not usually associated with this relaxation mechanism since nuclei close to the unpaired electron see a large local field and their resonance is shifted too far to be observable. Only those nuclei contribute to the resonance whose frequencies are sufficiently close for spin diffusion to take place. Thus if the shift and relaxation we have observed have the same source, localized paramagnetic centers are unlikely to be responsible.

Alternatively, if the unpaired electrons are delocalized, then the dominant relaxation would be the isotropic scalar coupling between the electron and nuclear spins, i.e., the contact hyperfine interaction:

$$H = \frac{8\pi}{3}\gamma_e\gamma_n\hbar^2\bar{\mathbf{I}}\cdot\bar{\mathbf{S}}\delta(\bar{\mathbf{r}}) \ , \tag{2}$$

where γ_e and γ_n denote the electronic and nuclear gyromagnetic ratios, respectively. The relaxation rate is given by[27]

$$T_1^{-1} = \tfrac{32}{9}\pi^2\gamma_e^2\gamma_n^2\hbar^4 J(\omega) \ , \tag{3}$$

where $J(\omega)$ is the spectral density associated with the fluctuating field experienced by the nuclei. For conduction electrons $J(\omega)$ reduces to[28]

$$J = \frac{2\pi}{\hbar}\int_0^\infty \langle\,|\psi(0)|^2\rangle_E^2\rho^2(E)f(E)[1-f(E)]dE \ , \tag{4}$$

where $\langle\,|\psi(0)|^2\rangle_E$ denotes the average density of the electronic wave functions with energy E at the nuclear position [$\psi(r)$ normalized per unit volume], $\rho(E)$ is the electronic density of states per direction of spin, and $f(E)$ is the probability that a state of energy E is occupied by an electron. For degenerate electrons obeying Fermi-Dirac statistics Eq. (4) becomes[28]

$$J = \frac{2\pi}{\hbar}\langle\,|\psi(0)|^2\rangle_{E_F}^2\rho^2(E_F)k_BT \ , \tag{5}$$

where E_F denotes the Fermi energy. Substitution of Eq. (5) into Eq. (3) gives

$$T_1^{-1} = \tfrac{64}{9}\pi^3\hbar^3\gamma_e^2\gamma_n^2\langle\,|\psi(0)|^2\rangle_{E_F}^2\rho^2(E_F)k_BT \ , \tag{6}$$

which, for a quasifree-electron gas, becomes[29]

$$T_1^{-1} = \tfrac{16}{9}(3\pi^2)^{2/3}\frac{\gamma_e^2\gamma_n^2}{\pi\hbar}\langle\,|\psi(0)|^2\rangle_{E_F}^2 m^{*2}n_e^{2/3}k_BT \ , \tag{7}$$

where χ_p is the electronic spin susceptibility per unit volume. Neglecting electron-electron interactions, the shift for quasifree electrons then becomes

$$K = \frac{\Delta H}{H_0} = \frac{8\pi}{3}\langle\,|\psi(0)|^2\rangle_{E_F}\chi_p \ , \tag{8}$$

where χ_p is the electronic spin susceptibility per unit volume. Neglecting electron-electron interactions, the shift for quasifree electrons then becomes

$$K = \frac{2(3\pi^2)^{1/3}}{3\pi}\gamma_e^2\langle\,|\psi(0)|^2\rangle_{E_F}m^*n_e^{1/3} \ . \tag{9}$$

Combination of Eq. (9) with Eq. (7) or Eq. (8) with Eq. (6) leads to the well-known Korringa relation for degenerate electrons[31]

$$K^2T_1T = \frac{\hbar}{4\pi k_B}\left[\frac{\gamma_e}{\gamma_n}\right]^2 \ . \tag{10}$$

Now the relaxation data shown in Fig. 2 could obviously be fit to Eq. (7) by assuming a particular temperature dependence of n_e. However, the Korringa relation, independent of n_e, provides a much more stringent test of the degenerate electron model. We find, in fact, that values of K^2T_1T determined from our measurements are two orders of magnitude smaller than predicted by Eq. (10) and they are strongly temperature dependent. This is true for any reasonable choice of zero for the resonance shift. Thus, contrary to the conclusion drawn by Tinelli and Holcomb,[15] we find that the observed relaxation is not consistent with relaxation by degenerate electrons.

In short, both the localized and degenerate-itinerant models discussed above fail to give either the correct magnitude or temperature dependence for the shift and relaxation. Increased dissolution of excess cesium into the impurity band at high temperatures might be able to provide the observed temperature dependences of K and T_1 on the degenerate-itinerant models, but it would not cause the large Korringa product variation that is observed.

A description which does give the correct magnitude and temperature dependence for all of these quantities is based on nondegenerate electrons obeying Boltzmann statistics. These might be, for example, electrons excited to the conduction band from excess-cesium donors. The wave-function density $\langle\,|\psi(0)|^2\rangle_E$ is a slowly varying function of E so that if $E-E_F \gg k_BT$, $1-f(E)\approx 1$ and Eq. (4) can now be written as

$$J = \frac{2\pi}{\hbar}\langle\,|\psi(0)|^2\rangle_{E_0}^2\int_{E_g}^\infty \rho^2(E)f(E)dE \ , \tag{11}$$

where E_0 is an energy near the bottom of the conduction band and E_g is the energy gap. Substituting the density of states for a parabolic band, we find

$$T_1^{-1} = \frac{32}{9}\frac{\gamma_e^2\gamma_n^2}{\pi\hbar^3}\langle\,|\psi(0)|^2\rangle_{E_0}^2 m^{*3}(k_BT)^2e^{-(E_g-E_F)/k_BT} \ . \tag{12}$$

Equation (12) suggests the semi-logarithmic plot of

$(T_1T^2)^{-1}$ versus $1/T$ in Fig. 4 which yields a good straight line, except at the lowest temperature where an additional relaxation mechanism may be present. The linear fit has a slope of 0.25 eV which is clearly less than the energy gap determined optically (>2.0 eV).

The resonance shift for nondegenerate electrons is proportional to the number of electrons n_e in the conduction band, i.e.,[32]

$$K=\frac{\Delta H}{H_0}=\frac{2\pi}{3}\gamma_e^2\hbar^2\langle\,|\psi(0)|^2\rangle_{E_0}\frac{n_e}{k_BT}\ . \tag{13}$$

The shift shown in Fig. 3 includes contributions from the chemical shift as well as from any unpaired electrons present. However, the chemical shift (which is roughly proportional to the inverse of the ionicity of the bond) should be only weakly temperature dependent and the rapidly rising shift at high temperature is consistent with an increasing number of electrons in the conduction band. One can often write the electron concentration as[33]

$$n_e=2(k_BT/2\pi\hbar^2)^{3/2}m^{*3/2}e^{-(E_g-E_F)/k_BT}\ , \tag{14}$$

and in this case the shift becomes

$$K=\frac{\Delta H}{H_0}=\tfrac{2}{3}(k_B/2\pi)^{1/2}\frac{\gamma_e^2}{\hbar}\langle\,|\psi(0)|^2\rangle_{E_0}\times m^{*3/2}T^{1/2}e^{-(E_g-E_F)/k_BT}\ . \tag{15}$$

By combining (12) and (15) we find the "Korringa relation" for nondegenerate electrons:

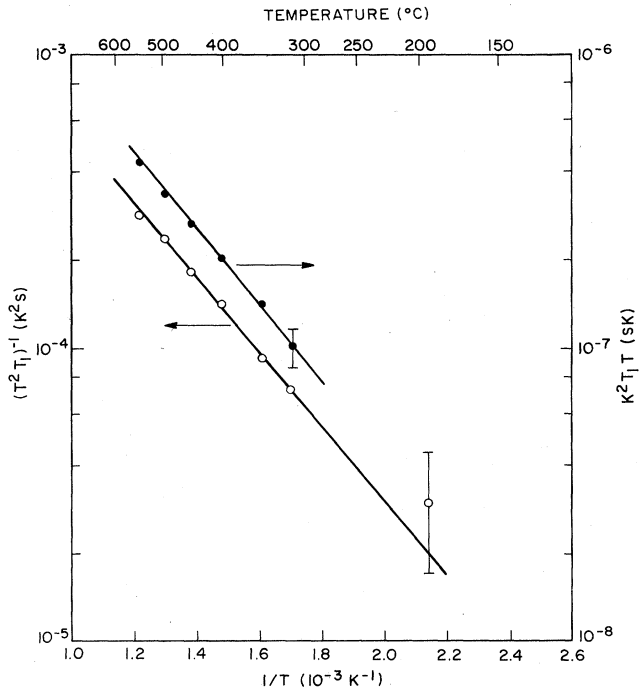

FIG. 4. Semilogarithmic plot of K^2T_1T (upper curve, right-hand scale) and $(T^2T_1)^{-1}$ (lower curve, left-hand scale) versus $1/T$ for ^{133}Cs in solid CsAu. Solid lines have slopes corresponding to $E_g-E_F=0.25$ eV in Eqs. (12) and (16).

$$K^2T_1T=\frac{\hbar}{16k_B}\left[\frac{\gamma_e}{\gamma_n}\right]^2e^{-(E_g-E_F)/k_BT}\ . \tag{16}$$

This is similar to the Korringa relation for degenerate electrons, but includes the exponential factor which depends upon the gap.

Figure 4 also shows a plot of K^2T_1T versus $1/T$, where we have taken the shift due to conduction electrons to be measured relative to $\Delta H/H_0=375$ ppm, the shift at room temperature. This plot gives a good straight line with the same slope as that of $(T_1T^2)^{-1}$ within the experimental error. The magnitude of K^2T_1T agrees well with Eq. (16). For $E_g-E_F=0.25$ eV, the experimental value of K^2T_1T corresponds to a prefactor 1.5×10^{-5} s K. This is to be compared with the value $(\hbar/16k_B)(\gamma_e/\gamma_n)^2=1.20\times10^{-5}$ s K from Eq. (16). Thus both the temperature dependences and the relative magnitudes of the shift and relaxation rate support their attribution to nondegenerate, delocalized electrons.

The electronic excitation energy 0.25 eV is much less than the band gap of CsAu. This suggests that these electrons are excited from impurity states lying 0.25 eV below the bottom of the conduction band. Although we are aware of no direct evidence, it is reasonable to suppose that these "impurities" are in fact equilibrium concentrations of excess Cs dissolved in CsAu. The constant presence of a weak, second ^{133}Cs NMR line is clear evidence that our samples always contained a small amount of second phase which, at high temperatures, could act as a source to maintain saturated Cs concentrations in the majority phase material. Below 300 °C, on the other hand, the electron concentration in the majority phase becomes dependent on small variations in sample composition suggesting that achievement of equilibrium concentrations is hindered by slow diffusion rates at low temperatures. We emphasize that these speculations are drawn from the phenomenology of the NMR results and that a deeper understanding of these effects must await the availability of details of the phase diagram very close to the stoichiometric composition.

B. Liquid CsAu

Nuclear relaxation in liquid CsAu is dominated by a different mechanism than the one we have postulated for the solid state. This is a central result of this work and may be seen directly from the very large increase in relaxation rate which occurs on melting but which is not accompanied by a similar increase in the shift. In general the relaxation rate due to unpaired electrons may be expressed as

$$1/T_1=B^2\langle\,|\psi(0)|^2\rangle^2\tau\ , \tag{17}$$

where B is a function of the number of electrons and τ is the correlation time characterizing fluctuations of the local hyperfine field. For a system of itinerant electrons, the correlation time need not appear explicitly in expressions such as Eq. (6) for the relaxation rate. In metals, for instance, $\tau\simeq\hbar N(E_F)$ and τ has a value on the order of 10^{-15} s, characteristic of the time a conduction electron spends near a particular nucleus. Now the shift is propor-

tional to $B\langle|\psi(0)|^2\rangle$ so that a large increase in relaxation rate unaccompanied by a change in shift must reflect a substantial increase in τ on melting. That is, the electrons become much more strongly localized in the liquid.

The structure of the localized states in the liquid was analyzed in our previous work.[16] We showed from an estimate of the hyperfine interaction strength, i.e., $\langle|\psi(0)|^2\rangle$, and the variation of $1/T_1$ with excess metal that the electrons are localized in states analogous to F centers. Thus the electronic charge is localized mainly off the metal ions and is shared by a coordinating shell of Cs^+ ions. The correlation times τ for these states are about 0.3 ps, somewhat shorter than a typical liquid-state ionic configuration but much longer than metallic values. Studies at various concentrations near stoichiometry suggest the presence of a concentration $n_e \simeq 4\times 10^{19}$ electrons/cm^3 in stoichiometric CsAu. The temperature dependence of the shift and relaxation rate in the liquid are consistent with thermal creation of F centers with an activation energy $\Delta E \sim 0.2$—0.3 eV.

C. Comparison of CsAu with other compounds

Since CsAu resembles in some respects both highly ionic compounds and typical semiconductors, it is instructive to compare the properties of CsAu with typical examples of these two classes of material. We consider first the ionic compounds exemplified by the alkali halides and, in particular, by CsI. The energy gap in CsI is sufficiently large (~ 6 eV) (Ref. 34) that there is essentially no electronic conduction in the pure compound. In contrast to CsAu, CsI can be prepared easily in highly stoichiometric form. In the liquid state of either compound, small amounts of excess metal introduce localized states analogous to F centers.[24,35,36] But the lifetimes of the states inferred from nuclear hyperfine correlation times differ by roughly an order of magnitude. This time is about 2 ps for CsI containing less than 1 mol % excess Cs (Ref. 24) compared with 0.3 ps in CsAu near stoichiometry.[16] In the solid state, excess metal also introduces F centers in CsI, but in CsAu an impurity band is formed. This leads to significantly different high-temperature electronic properties for the two systems. A further difference, presumably related to the larger band gap of CsI, is the absence of thermally generated localized paramagnetic centers in stoichiometric liquid CsI.

For highly covalent semiconductors such as the III-V compounds, melting produces essentially complete destruction of the chemical bond and metallic behavior develops immediately on melting.[37] More ionic semiconductors such as the II-VI and III-VI compounds exhibit intermediate behavior. These materials tend to become poor metals or liquid semiconductors just above the melting point and they gradually evolve toward a more metallic state on further heating.[37] Thus while the solid-state behavior of the covalent compounds is not unlike that of CsAu, they do not melt to an ionic liquid state. CuI_2, which has a solid-state energy gap similar to CsAu (2.8 eV), is the only other example known to us of a compound showing a melting transition from solid semiconductor to ionic liquid.[38]

V. SUMMARY

Our NMR measurements of solid CsAu at elevated temperatures yield a strongly-temperature-dependent nuclear relaxation rate accompanied by a more weakly-temperature-dependent resonance shift. We have interpreted this behavior as evidence for electrons excited into the conduction band where they are delocalized. The source of these electrons may be a donor band due to excess cesium which is located about 0.25 eV below the conduction band.

The character of the states occupied by these electrons changes significantly when the crystal melts. Since ionic melts typically maintain a high degree of short-range compositional order, the melting transition mainly involves a loss of long-range order. Our results indicate that the itinerant conduction electron states can no longer be supported by the disordered liquid structure and the electrons localize in sites where they are surrounded by several metal ions.

ACKNOWLEDGMENTS

The authors wish to express their appreciation to W. Freyland for several valuable discussions and for his help and guidance in the preparation of samples and cells. We are grateful to D. Hamann for an illuminating discussion and for permission to refer to unpublished band-structure calculations for CsAu. G. F. Brennert provided expert technical assistance, particularly in the preparation of samples at AT&T Bell Laboratories and D. W. Murphy generously made available his dry-box facility for this purpose. We wish to thank the Science and Engineering Reserach Council (U.K.) for their support of the Warwick portion of this work.

*Present address: Thor Cryogenics, Berinsfield, Oxfordshire, England.

[1]H. Hoshino, R. W. Schmutzler, and F. Hensel, Phys. Lett. **51A**, 7 (1975).

[2]R. W. Schmutzler, H. Hoshino, R. Fischer, and F. Hensel, Ber. Bunsenges. Phys. Chem. **80**, 197 (1976).

[3]K. D. Kruger and R. W. Schmutzler, Ber. Bunsenges. Phys. Chem. **80**, 816 (1976).

[4]W. Freyland and G. Steinleitner, Ber. Bunsenges. Phys. Chem. **80**, 810 (1976).

[5]W. Martin, W. Freyland, P. Lamparter, and S. Steeb, Phys. Chem. Liquid **10**, 61 (1980).

[6]A. Kempf and R. W. Schmutzler, Ber. Bunsenges. Phys. Chem. **84**, 5 (1980).

[7]F. Sommer, D. Eschenweck, B. Predel, and R. W. Schmutzler, J. Met. **32**, 3 (1980).

[8]M. A. Bredig, in *Molten Salt Chemistry,* edited by M. Blander (Interscience, New York, 1964), p. 367.
[9]G. Kienast and J. Verma, Z. Anorg. Allg. Chem. **310**, 143 (1961).
[10]W. E. Spicer, A. H. Sommer, and J. E. White, Phys. Rev. **115**, 57 (1959).
[11]A. Hasegawa and M. Watabe, J. Phys. F **7**, 75 (1977).
[12]H. Overhof, J. Knecht, R. Fischer, and F. Hensel, J. Phys. F **8**, 1607 (1978).
[13]D. R. Hamann and M. Schluter (unpublished).
[14]F. Wooten and G. A. Condas, Phys. Rev. **131**, 657 (1963).
[15]G. A. Tinelli and D. F. Holcomb, J. Solid State Chem. **25**, 157 (1978).
[16]R. Dupree, D. J. Kirby, W. Freyland, and W. W. Warren, Jr., Phys. Rev. Lett. **45**, 130 (1980).
[17]W. G. Clark, Rev. Sci. Instrum. **35**, 316 (1964).
[18]C. Deverell and R. F. Richards, Mol. Phys. **10**, 551 (1966).
[19]D. J. Kirby, Ph.D. thesis, U. Warwick, 1981 (unpublished).
[20]U. El-Hanany and W. W. Warren, Jr., Phys. Rev. B **12**, 861 (1975).
[21]Sauereisen No. 4, Sauereisen Cements Col., Pittsburgh, Pennsylvania.
[22]D. I. Hoult, Prog. Nucl. Magn. Reson. Spectrosc. **12**, 41 (1978).
[23]A. R. Haase, M. A. Kerber, D. Kessler, J. Kronenbitter, H. Krüger, O. Lutz, M. Müller, and A. Nolle, Z. Naturforsch. **32a**, 952 (1977).
[24]W. W. Warren, Jr., S. Sotier, and G. F. Brennert, Phys. Rev. B **30**, 65 (1984).
[25]A. Abragam, *Principles of Nuclear Magnetism* (Oxford, London, 1961), p. 378ff.
[26]A. Abragam, *Principles of Nuclear Magnetism,* Ref. 25, p. 382.
[27]A. Abragam, *Principles of Nuclear Magnetism,* Ref. 25, p. 310.
[28]C. P. Slichter, *Principles of Magnetic Resonance* (Harper and Row, New York, 1963), p. 123.
[29]The derivation here of Eqs. (7)—(16) generally follows a similar derivation by H. Selbach, O. Kanert, and D. Wolf, Phys. Rev. B **19**, 4435 (1979). Their paper, however, contains a number of numerical and typographical errors which we have corrected in the present work.
[30]C. H. Townes, C. Herring, and W. D. Knight, Phys. Rev. **77**, 852 (1950).
[31]J. Korringa, Physica (Utrecht) **16**, 601 (1950).
[32]Equation (13) is obtained by substituting the Curie susceptibility of n_e spin $\frac{1}{2}$ particles, $\chi = n_e \gamma_e^2 \hbar^2 / 4 k_B T$, into Eq. (8). The expression differs by a factor of 4 from the one originally given by N. Bloembergen, Physica (Utrecht) **20**, 1130 (1954), apparently obtained with an approximate form of the electronic susceptibility.
[33]J. M. Ziman, *Principles of the Theory of Solids* (Cambridge, London, 1964), p. 122.
[34]See, for example, K. Teegarden and G. Baldini, Phys. Rev. **155**, 896 (1967).
[35]S. Sotier and W. W. Warren, Jr., J. Phys. (Paris) **41**, C8-40 (1980).
[36]W. W. Warren, Jr. and S. Sotier, in *Proceedings of the Third International Symposium on Molten Salts,* edited by G. Mamantov, M. Blander, and G. P. Smith (Electrochemical Soceity, Princeton, 1981), p. 95.
[37]See, for example, V. M. Glazov, S. N. Chizhevskaya, and N. N. Glagoleva, *Liquid Semiconductors* (Plenum, New York, 1969).
[38]See, for example, F. Hensel, Adv. Phys. **28**, 555 (1979).